

TikArt: Aperture-Guided Observation for Fine-Grained Visual Reasoning via Reinforcement Learning

Hao Ding^{1*}, Zhichuan Yang^{2*}, Weijie Ge³, Ziqin Gao¹, Chaoyi Lu², Lei Zhao^{1†}

¹Zhejiang University, ²Xi'an Jiaotong University,
³Zhejiang University of Science and Technology

Abstract

We address fine-grained visual reasoning in multimodal large language models (MLLMs), where key evidence may reside in tiny objects, cluttered regions, or subtle markings that are lost under a single global image encoding. We introduce TikArt (Thinking Aperture), an aperture-guided agent that casts multi-step vision-language reasoning as a decision process over regions of interest. TikArt follows a Think-Aperture-Observe loop, alternating between language generation and two aperture actions: Zoom extracts rectangular crops, while Segment invokes SAM2 to obtain mask-based crops for irregular targets. After every action, the model must produce an explicit observation, turning local visual cues into persistent linguistic memory. Built on Qwen3-VL-8B, TikArt optimizes its reasoning policy with AGRPO, a GRPO-style reinforcement learning algorithm with a two-stage curriculum: it warms up segmentation actions and then jointly optimizes visual math, fine-grained VQA, and segmentation, using rewards that couple task success with purposeful aperture use. Experiments on V*, HR-Bench-4K/8K, MME-RealWorld-Lite, MMStar, RefCOCO, and ReasonSeg show consistent gains over the backbone and yield interpretable aperture trajectories for high-resolution reasoning.

1 Introduction

Multimodal large language models (MLLMs) like GPT4o, QwenVL series, Gemini family and internVL (Bai et al., 2023; OpenAI, 2024; Team et al., 2024; Wang et al., 2025c) have achieved strong performance on general vision-language tasks such as open-domain VQA, captioning, and image-grounded dialogue. Yet they still struggle with *fine-grained* visual reasoning. When crucial

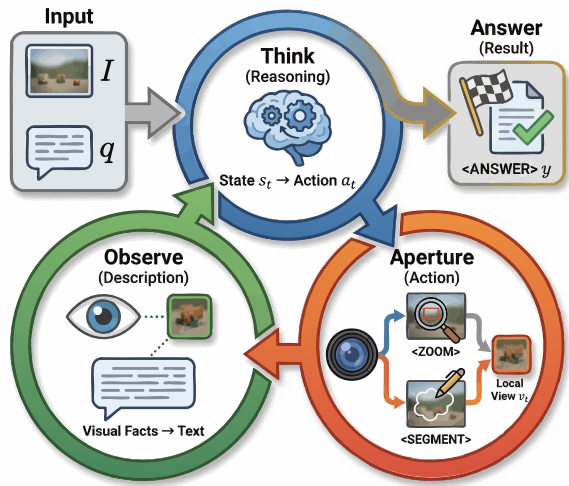


Figure 1: The TikArt Framework. The model employs a Think-Aperture-Observe (TAO) Loop to iteratively perceive fine-grained visual details (v_t) before generating the final answer.

evidence lies in tiny objects, faint textures, symbolic marks, or partially occluded regions, mainstream MLLMs typically process the whole image once into a fixed set of visual tokens and then reason purely in the text domain. Visual evidence becomes effectively *static* along the chain-of-thought, and the model can only reweight a coarse global representation instead of actively revisiting informative details. High-resolution benchmarks such as V* (Wu and Xie, 2024) and HR-Bench (Wang et al., 2025d), together with reasoning-style segmentation and visual math tasks, show that simply scaling model size or context length is insufficient to close this gap.

Humans, in contrast, seldom rely on a single global snapshot. We naturally move our gaze across *regions of interest* (RoIs), alternating between deciding *where to look* and interpreting *what we see*. Each fixation reveals new local evidence that influences the next decision, forming a sequential, interactive process. Inspired by this perspec-

* Equal contribution.

† Corresponding author.

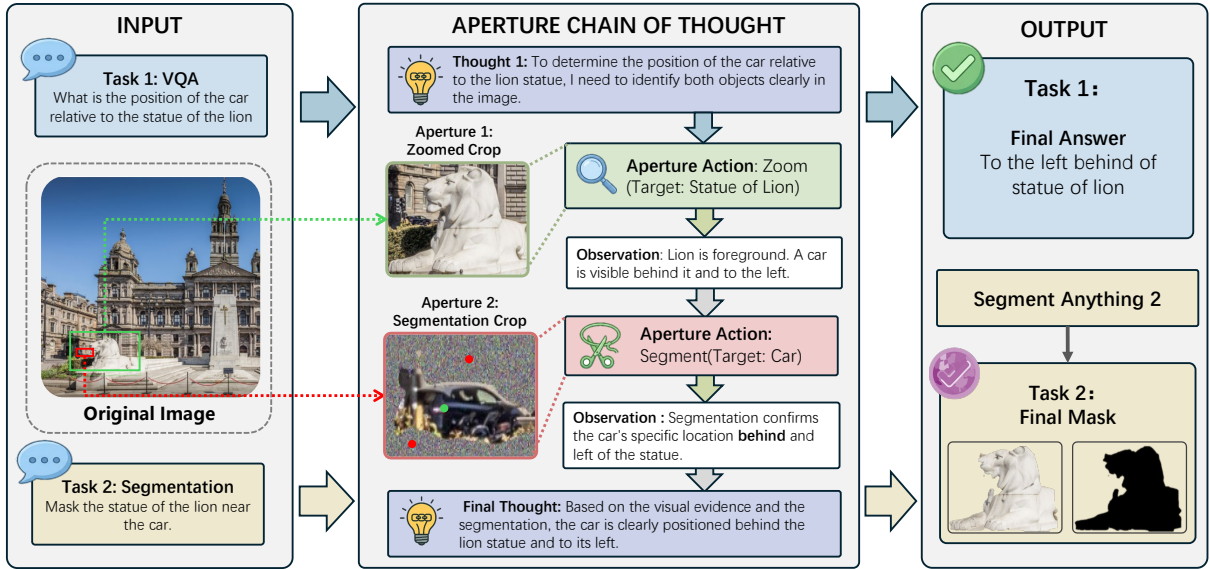


Figure 2: TikArt performs aperture-guided observation across modalities. A single reasoning trajectory alternates between selecting regions of interest (RoIs) and describing what is seen there. In the example, the same sequence of aperture decisions supports a spatial VQA query (blue arrows) and a segmentation instruction (yellow arrows), while the dashed links indicate the underlying high-resolution image from which RoIs are extracted and refined. Segmentation masks are obtained by SAM2(Ravi et al., 2024).

tive, we introduce the notion of an *aperture*: a localized ROI crop that serves as a controllable window of visual focus. Reasoning then becomes a process of “thinking in apertures”: the agent repeatedly selects apertures on the image and updates its beliefs based on what is observed there.

Recent work on “thinking with images” has begun to expose similar behaviors in MLLMs by interleaving visual operations with textual reasoning (Zheng et al., 2025; Hong et al., 2025). However, existing systems often rely on fixed workflows or loosely coupled external modules, and their visual operations are not tightly integrated with the internal decision-making process. A critical interface is often under-specified: after a visual action is taken, how is the newly acquired evidence explicitly committed into subsequent reasoning in a grounded, reusable, and human-auditable manner? If the outcome of an action remains latent (e.g., repeated crops/segmentations without an explicit evidence statement), the reasoning trace becomes difficult to audit, and learning signals become weakly coupled to what the model actually extracted. This leaves two questions underexplored: (i) how to cast multimodal reasoning itself as a decision process over RoIs, and (ii) how to ensure that each

visual decision is grounded by an explicit, human-interpretable observation rather than being a latent, opaque operation. Addressing these questions naturally calls for two coupled components: an aperture policy that decides where and how to look, and an observation policy that decides what to state about the selected region.

In this work, we address these questions with **TikArt**. We call the resulting interleaved sequence of apertures and observations an **Aperture Chain-of-Thought (A-CoT)**. We view interleaved multi-step visual reasoning (Trivedi et al., 2023; Gao et al., 2025; Chen et al., 2025) as a Markov Decision Process (MDP) (Puterman, 1990) over RoIs: at each step, an agent observes the current multimodal state (image, question, textual history, and previously inspected apertures), chooses an *aperture action* that selects or refines a region of interest, and then produces a natural-language *observation* describing the newly obtained visual evidence. Crucially, TikArt enforces a *mandatory Observation phase* after every aperture action: the model must explicitly describe what appears in the selected region before proceeding. These observations are appended to the chain-of-thought, turning local visual cues into persistent linguistic memory. This

yields a Think–Aperture–Observe loop in which the agent must decide *when* to look again, *where* to place the next aperture, and *how* to verbalize what it perceives before committing to an answer.

Within this framework, TikArt learns two primitive aperture actions that resemble human eye and hand movements. A *zoom* action extracts a bounded ROI, akin to directing foveal vision toward a particular icon, formula panel, or table cell. A *segmentation* action isolates irregular or cluttered foreground regions via mask-based cropping, similar to mentally tracing the outline of an object or group of objects; in practice, this is realized by invoking a segmentation module such as SAM2. From the agent’s perspective, both are unified as ROI-centric decisions about where and how to focus, and both must be justified by the subsequent observation.

TikArt instantiates this aperture-guided observation paradigm on Qwen3-VL-8B (Bai et al., 2025). Rather than supervising explicit chains of thought or hand-crafted aperture traces, we adopt a dual-stage reinforcement learning (RL) pipeline based on Group Relative Policy Optimization(GRPO) (Shao et al., 2024) without intermediate supervised fine-tuning (SFT), thereby avoiding dependence on scarce high-quality image-conditioned chain-of-thought data. The first stage emphasizes visually grounded behaviors, and the second applies multi-task RL over visual math, fine-grained VQA, and segmentation. Importantly, we also report a training-free prompt-only variant (w/o GRPO) that directly applies the same Think–Aperture–Observe prompting to the backbone at inference time. It already yields non-trivial gains, while full AGRPO further improves the aperture policy and can be more latency-efficient (Appendix A). Ablations (Sec. 4.5) show that removing either aperture actions or the Observation phase leads to unstable training and clear drops in high-resolution perception, highlighting that observation is not merely explanatory but central to the decision process.

Extensive experiments demonstrate that aperture-guided observation substantially improves fine-grained visual reasoning. On V* and HR-Bench 4K/8K, TikArt-8B achieves large gains over its Qwen3-VL-8B-Instruct backbone (e.g., double-digit improvements on V* and HR-Bench-8K), approaches or even surpasses larger open-source models such as Qwen3-VL-32B and 235B, and matches or outperforms strong proprietary sys-

tems (e.g., GPT-5 (OpenAI, 2025), Gemini-2.5 (Comanici et al., 2025)) on the most challenging high-resolution settings under our standardized evaluation. On MME-RealWorld-Lite (Zhang et al., 2024) and MMStar (Chen et al., 2024), TikArt consistently improves perception and reasoning scores and narrows the gap to GPT-4o and Gemini-2.5 while remaining significantly stronger than 8B-scale baselines. Beyond recognition-style benchmarks, TikArt attains competitive performance on RefCOCO (Yu et al., 2016) and exhibits particularly strong gains on the reasoning-oriented ReasonSeg benchmark (Lai et al., 2024), indicating that the same ROI-centric decision policy naturally extends from question answering to pixel-level grounding. We also report aperture-usage statistics and inference latency for both training-free and RL-trained variants to characterize the accuracy–cost trade-off of iterative perception (Appendix A).

Our contributions are threefold:

1. We identify fine-grained visual reasoning under high-resolution inputs as a core bottleneck of current MLLMs and empirically show that strong proprietary and open-source models still struggle when critical evidence is localized in small or complex regions.
2. We propose **aperture-guided observation**, which formalizes multimodal reasoning as an MDP over regions of interest with a Think–Aperture–Observe loop, explicitly separating an aperture policy (where and how to look) from an observation policy (what to verbalize about what is seen and commit into text).
3. We develop and train **TikArt**, an aperture-guided agent built on Qwen3-VL-8B and optimized via a dual-stage, GRPO-style reinforcement learning pipeline without SFT. TikArt learns to coordinate **zoom** and **segmentation** aperture actions and their associated observations without chain-of-thought supervision, and we additionally report a training-free prompt-only variant (w/o GRPO) to isolate the effect of the prompting/interface from RL, yielding consistent gains with interpretable aperture trajectories.

2 Related Work

Segment Models Foundation segmentation models aim to provide open-vocabulary, high-quality masks with flexible prompting. Segment Anything

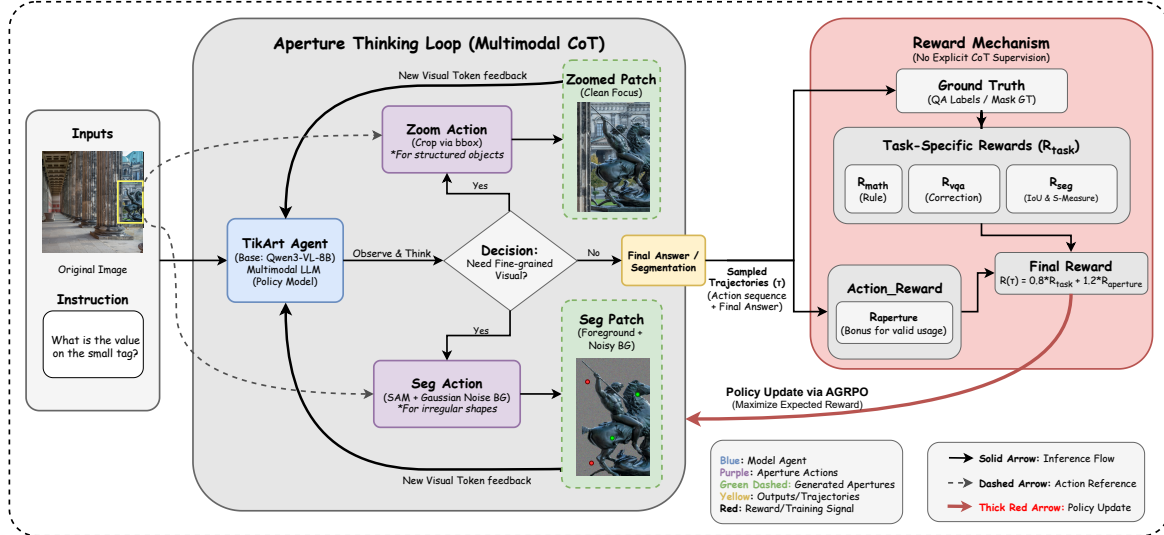


Figure 3: Overview of TikArt Framework. TikArt unifies token-level reasoning, visual aperture generation, and reinforcement learning signals. The model alternates between language generation and action invocation (Zoom/Segment) to form an aperture trajectory, while AGRPO provides task and action rewards to shape aperture-guided reasoning.

(SAM) (Kirillov et al., 2023) trains a ViT-based image encoder with a lightweight mask decoder over large-scale mask data, framing segmentation as a unified “promptable” task (e.g., point/box-/mask prompts) that generalizes widely in a zero-shot manner (Kirillov et al., 2023). SAM2 extends this paradigm to video, introducing streaming memory and a data engine for scalable video segmentation, enabling interactive, temporally consistent segmentation across frames. LISA (Lai et al., 2024) has connected the segment tasks with MLLMs and realizes end-to-end segmentation using large language models (LLMs). More recently, reinforcement learning has been explored to strengthen such segmentation-capable multimodal systems. Seg-R1 applies GRPO-style RL to train an LMM to generate spatial prompts (points/boxes) that guide SAM2, demonstrating strong transfer to referring/reasoning segmentation despite limited training supervision (You and Wu, 2025)

MLLMs and Visual Reasoning Evolved from foundation MLLMs, Tool augmentation offers a practical route to overcome static visual representations by allowing models to act (call tools) between reasoning steps. In text-only settings, ReAct interleaves explicit reasoning traces with actions (e.g., API calls), improving both performance and interpretability (Yao et al., 2023). This idea naturally extends to multimodal systems. MM-ReAct generalizes ReAct to multimodality by composing a pool

of vision experts, allowing the LLM to request specialist perception when needed for advanced visual understanding (Yang et al., 2023). A newer wave of “think-with-image” methods makes iterative visual operations part of the reasoning loop. (Hu et al., 2024; Su et al., 2025; Yu et al., 2025b) With the advancement of reinforcement learning (RL) in LLMs like GRPO, DeepEyes likewise explores multi-step, query-oriented visual reasoning with iterative “look closer” style operations, strengthening fine-grained perception during inference. Inspired by existing works, we propose **TikArt**, which combines the segment models in **Visual Reasoning**.

3 Method

TikArt equips Qwen3-VL-8B (Bai et al., 2025) with *aperture-guided* visual interaction, allowing the model to dynamically reasoning. As illustrated in Fig. 3, the model interleaves language reasoning with aperture actions that extract local visual evidence, forming a unified *Aperture Chain-of-Thought* (A-CoT). The improvements in Table 1 and Table 2 demonstrate that explicit aperture control is highly beneficial for high-resolution perception and multimodal reasoning.

3.1 A-CoT as a Markov Decision Process

Given an image I and query q , TikArt generates a sequence of actions from a combined vocabulary $\mathcal{V} \cup \mathcal{T}$, where \mathcal{V} is the text token vocabulary

Model	Params	V*			HR Bench 4K			HR Bench 8K		
		Attr	Spatial	Overall	FSP	FCP	Overall	FSP	FCP	Overall
Proprietary models										
GPT-4o	-	71.30*	69.74*	70.68*	68.75*	59.00*	63.87*	60.75*	60.00*	60.38*
GPT-5	-	74.78	78.95	76.44	78.00	77.00	77.50	70.50	72.75	71.62
GPT-5-nano	-	58.26	72.37	63.87	69.00	61.75	65.38	65.75	61.50	63.63
Gemini-2.5-pro	-	84.35	71.05	79.06	88.75	87.00	87.87	84.50	82.75	83.62
Gemini-2.5-flash	-	84.35	73.68	80.10	85.00	77.00	81.00	79.00	73.50	76.25
Visual Reasoning Models										
Pixel-Reasoner (Wang et al., 2025a)	7B	-	-	84.30*	-	-	74.00*	-	-	66.90*
Thyme (Zhang et al., 2025)	7B	-	-	82.20*	-	-	77.00*	-	-	72.00*
LVR (Li et al., 2025)	7B	81.7*	79.0*	80.6*	-	-	-	-	-	-
Deepeyes	7B	84.35*	81.58*	83.03*	83.75*	58.74*	71.25*	77.00*	53.25*	65.13*
Monet-7B (Wang et al., 2025b)	7B	83.48*	82.89*	83.25*	85.25*	56.75*	71.00*	79.75*	56.25*	68.00*
Open-source models										
LLaVA-OneVision-1.5	8B	83.48	85.53	84.29	72.00	46.50	59.25	59.50	43.75	51.62
Qwen3-VL-235B-A22B-Instruct	235B [†]	88.50	78.95	84.66	90.50	71.75	81.13	82.25	70.00	76.13
Qwen3-VL-Instruct	32B	84.35	85.53	84.82	90.50	69.00	79.75	84.75	68.00	76.38
Qwen3-VL-Thinking	8B	71.30	75.00	72.77	81.00	60.00	70.50	73.75	60.50	67.13
Qwen3-VL-Instruct	8B	73.04	73.68	73.82	90.50	57.75	74.13	81.25	55.75	68.50
Fusion experiments (ours)										
TikArt	8B	91.30	86.84	89.53	93.75	70.75	82.25	84.50	68.25	76.38
Δ (vs Qwen3-VL-8B-Instruct)		+18.3	+13.2	+15.7	+3.3	+13.0	+8.1	+3.3	+12.5	+7.9
w/o Observation		89.57	81.58	86.39	94.00	67.25	80.63	85.25	64.75	75.00
w/o Zoom Action		76.32	86.42	80.34	93.75	65.25	79.50	85.25	64.25	74.75
w/o Segment Action		82.60	84.21	83.24	93.25	59.75	76.50	89.25	61.50	75.38
w/o GRPO		78.26	71.05	75.39	92.00	70.25	81.13	76.50	70.25	73.38

Table 1: Results on high-resolution perception benchmarks V*, HR Bench 4K and HR Bench 8K. TikArt greatly improves V* and HR-Bench 4K/8K over Qwen3-VL-8B-Instruct and narrows the gap to Qwen3-VL-32B/235B and GPT-5/Gemini-2.5. Values with * are taken from (Wang et al., 2025b; Hong et al., 2025). The best result in each column is in **bold** and the second best is underlined. “Params” denotes model parameter size. Ablations (w/o ·) remove one component/action and are trained unless stated otherwise; w/o GRPO is prompt-only (training-free), evaluated under the same inference setup. The green row (Δ) reports the absolute improvement of TikArt over Qwen3-VL-8B-Instruct. [†] denotes MoE model with 235B total params and 22B active params per token.

and \mathcal{T} contains decision tokens such as `<ZOOM>`, `<SEGMENT>`, and `<ANSWER>`. Each inference step corresponds to a transition in an MDP.

The multimodal state at time t is:

$$s_t = (I, q, h_{t-1}, \mathcal{A}_{1:t-1}), \quad (1)$$

where h_{t-1} is the partially generated A-CoT, and $\mathcal{A}_{1:t-1}$ denotes all previously extracted apertures (RoIs). A full rollout is:

$$\tau = \{(s_t, a_t, v_t)\}_{t=1}^T, \quad (2)$$

where a_t is the token-level action and v_t is either a Zoom crop, a segmentation-based local view, or a null view when no aperture is applied.

TikArt follows a structured reasoning loop:

Think → **Aperture** → **Observe** → ⋯ → **Answer**.

Unlike static single-pass vision encoders, this loop enables active perception and dynamic state transitions driven by visual exploration.

3.2 Mandatory Observation: Grounding What the Model Sees

A defining element of TikArt is the **mandatory Observation phase** triggered after every aperture

action. Once the local view v_t is obtained, the model must output a natural-language description of its content. This mechanism is crucial:

Grounded aperture usage. Observation forces the model to explicitly describe what appears inside the aperture—tiny characters, contour edges, symbolic strokes, or small object instances—ensuring that aperture actions meaningfully contribute to reasoning.

Converting visual cues into persistent memory. Fine-grained details may be lost in visual embeddings; verbalizing them turns local cues into stable linguistic memory for subsequent steps.

Improved reinforcement learning stability. During AGRPO, poor apertures lead to vague or incorrect observations, lowering return. Thus, Observation provides a tight perception–reward link: good apertures facilitate accurate descriptions, which in turn correlate with task success. The ablations in Table 1 and Table 2 confirm its necessity.

3.3 Visual Apertures

Apertures act as explicit visual actions that control where the model looks.

Zoom. For structured regions, TikArt predicts a bounding box:

$$b_t = (x_1, y_1, x_2, y_2) \in [0, 1000]^4, \quad (3)$$

which defines the crop v_t^{zoom} .

Segmentation (via SAM2). For irregular or cluttered scenes, TikArt predicts (b_t, p_t, ℓ_t) as input to SAM2 to obtain a binary mask M_t . The final aperture view is:

$$v_t^{\text{seg}} = M_t \odot I + (1 - M_t) \odot N, \quad (4)$$

where N is Gaussian noise, suppressing background distraction and highlighting foreground geometry.

3.4 AGRPO: Reinforcement Learning for Aperture Reasoning

The TikArt policy is jointly optimized using *AGRPO*, a GRPO-based reinforcement learner with token-level credit assignment. No chain-of-thought or action labels are provided; aperture usage and observation behaviors emerge from reward optimization. AGRPO shares several hyperparameters (clip-higher, $\beta_{KL} = 0$) with the DAPO(Yu et al., 2025a) variant of GRPO used in prior work, and differs mainly in its aperture-aware action space and reward shaping; additional implementation details are given in the experimental setup.

The optimization objective is:

$$\max_{\theta} \mathbb{E}_{\tau \sim \pi_{\theta}} [R_{\text{final}}(\tau)]. \quad (5)$$

Multiple rollouts per prompt form a group baseline, while the clip-higher mechanism encourages trajectories with high final reward. Since AGRPO assigns advantages at the token level, it teaches the policy *when* to look, *where* to look, and *how* to describe what is seen.

3.5 Two-Stage Training Strategy

Directly learning aperture reasoning from scratch is unstable. Segmentation mistakes early in training produce misleading visual states, leading the policy to avoid aperture usage altogether. TikArt therefore adopts a two-stage curriculum. Fig 4

Stage I: Segmentation warm-up. The model is first trained solely on segmentation-style data to learn reliable box/point/label predictions for SAM2. This stabilizes the aperture-extraction process so that segmentation views are meaningful rather than

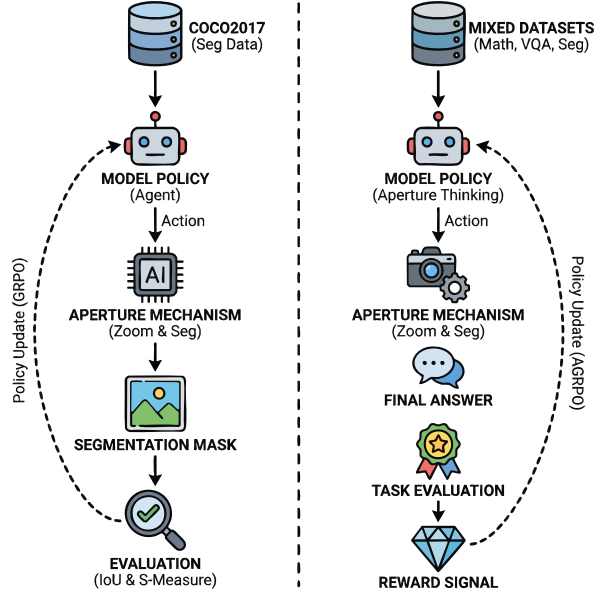


Figure 4: Two-stage training pipeline of TikArt. Stage 1 warms up the Segmentation action head to produce reliable foreground masks. Stage 2 applies multi-task AGRPO over visual math, fine-grained VQA, and segmentation tasks to learn aperture-guided reasoning.

noisy, and narrows the early action space, reducing the difficulty of RL exploration.

Stage II: Multi-task AGRPO. The model is then trained on mixed tasks including visual math, fine-grained VQA, and segmentation scenarios. This stage teaches the model to choose between Zoom and Segmentation, integrate observations into long-horizon reasoning, and form coherent A-CoT traces. The curriculum prevents reward hacking and leads to a stable aperture-usage policy.

3.6 Reward Design

TikArt’s final reward combines task success and meaningful aperture usage:

$$R_{\text{final}}(\tau) = \beta_1 R_{\text{task}}(\tau) + \beta_2 R_{\text{aperture}}(\tau), \quad (6)$$

where $\beta_1, \beta_2 > 0$ control the trade-off between task performance and aperture usage. In our experiments, we set $\beta_1 = 0.8$ and $\beta_2 = 1.2$. We include an alternative reward weighting ($\beta_1 = 1.0, \beta_2 = 0.8$) in the action count curve in Fig. 5b. Setting $\beta_2 < \beta_1$ leads to a rapid drop in aperture usage and performance, indicating that insufficient aperture incentives cause the model to underutilize visual actions.

Task reward. For visual math and VQA, $R_{\text{task}} \in \{0, 1\}$ is based on answer correctness. For segmentation, we use a continuous reward defined as a con-

Model	Params	MME-RealWorld-Lite		MMStar
		Perc.	Reas.	
Proprietary models				
GPT-4o	-	49.81	53.89	45.73
GPT-5	-	56.94	55.47	56.22
GPT-5-nano	-	46.11	49.40	42.82
Gemini-2.5-pro	-	52.10	50.73	53.48
Gemini-2.5-flash	-	49.70	47.32	52.07
Open-source models				
LLaVA-OneVision-1.5	8B	38.69	36.53	37.61
DeepEyes	7B	55.30	46.29	50.79
Monet-7B	7B	58.34*	51.07*	55.50*
Qwen3-VL-Instruct	235B [†]	56.30	60.78	51.82
Qwen3-VL-Instruct	32B	45.07	51.07	39.07
Qwen3-VL-Thinking	8B	44.05	34.80	39.43
Qwen3-VL-Instruct	8B	49.02	34.27	41.64
Fusion experiments (ours)				
TikArt	8B	60.48	53.47	56.97
Δ (Qwen3-VL-Instruct)		+11.5	+19.2	+15.3
w/o Observation		58.43	48.91	53.67
w/o Zoom Action		57.91	47.20	52.56
w/o Segment Action		53.51	47.87	50.69
w/o GRPO		50.65	46.55	48.60

Table 2: Results on MME-RealWorld-Lite and MMStar. TikArt narrows the gap to strong proprietary systems. Ablation settings are the same as in Table 1. “Perc.”, “Reas.” and “All.” denote Perception, Reasoning and Overall scores, respectively; Values with * are from (Wang et al., 2025b); † denotes MoE models.

vex combination of the IoU- and S-measure-based scores (Fan et al., 2017):

$$R_{\text{seg}} = (1 - \alpha) R_{\text{IoU}} + \alpha R_S, \quad (7)$$

where R_{IoU} and R_S denote the IoU and S-measure scores, respectively. We set $\alpha = 0.3$ in our experiments. To discard extremely low-quality segmentations, we further clip this reward by setting $R_{\text{seg}} = 0$ whenever the computed value falls below 0.1.

Aperture reward. The aperture reward $R_{\text{aperture}}(\tau) \in \{0, 1\}$ encourages purposeful aperture usage: it is set to 1 only when the trajectory both invokes at least one aperture action and achieves $R_{\text{task}}(\tau) > 0.3$, and 0 otherwise.

4 Experiments and Ablations

4.1 Experimental Setup

Benchmarks. We evaluate TikArt on four families of tasks: (1) high-resolution fine-grained reasoning on V*, MME-RealWorld-Lite and HR-Bench 4K/8K; (2) general multimodal understanding on MMStar; (3) referring segmentation on RefCOCO; and (4) reasoning-oriented segmentation on ReasonSeg. These benchmarks collectively cover small-object perception, spatial reasoning, real-world understanding, and pixel-level grounding.

Model	Params	RefCOCO		ReasonSeg-test	
		val	testa	testb	giou
Grounded SAM	-	-	-	-	21.3*
LISA	13B	74.9*	79.1*	72.4*	61.3*
SegR1	7B	74.3*	78.7*	67.6*	56.7*
VisionReasoner	7B	-	-	-	53.7*
SAM-R1	7B	79.2*	-	-	63.6*
TikArt	8B	77.1	79.6	69.1	73.8
w/o Observation		74.1	75.4	66.1	70.0
w/o Zoom Action		74.9	82.3	73.3	67.2
w/o Aperture		73.8	74.2	64.2	69.6

Table 3: Results on referring segmentation and reasoning segmentation benchmarks. TikArt brings ReasonSeg performance up to or beyond RL segmentation baselines while retaining strong RefCOCO scores. Values marked with * are taken from prior work (Lai et al., 2024; You and Wu, 2025; Huang et al., 2025). The best result in each column is shown in **bold**. TikArt w/o Aperture disables aperture control; w/o Zoom Action disallows the zoom action; w/o Observation removes the observation module.

Models and baselines. TikArt is built on Qwen3-VL-8B-Instruct and compared against its backbone, larger open-source models (LLaVA-OneVision-1.5-8B (An et al., 2025), Qwen3-VL-32B/235B), and strong proprietary systems (GPT-4o, GPT-5, GPT-5-nano, Gemini-2.5-Pro/Flash). All models are evaluated under a unified API-style setting with identical prompts and, for closed-source models, the same preprocessed images to ensure a fair comparison.

Prompt protocol. All evaluations use identical task prompts; differences are limited to a fixed tool-control prompt required for tool calls (Appendix E). DeepEyes follows its official prompt.

4.2 High-Resolution Fine-Grained Reasoning

Table 1 summarizes results on V* and HR-Bench 4K/8K. TikArt-8B delivers substantial gains over its Qwen3-VL-8B backbone, improving the overall V* score by around +15 points and HR-Bench 8K by roughly +8 points. Under the same evaluation protocol, TikArt-8B approaches or even surpasses Qwen3-VL-32B and 235B on several metrics, and matches or outperforms GPT-5 and Gemini-2.5 on the most challenging 8K settings, despite using a significantly smaller backbone.

4.3 Real-World Multimodal Benchmarks

On the high-resolution real-world benchmark MME-RealWorld-Lite and the broader MMStar suite (Table 2), TikArt consistently improves over Qwen3-VL-8B-Instruct across both perception and reasoning dimensions. While proprietary mod-

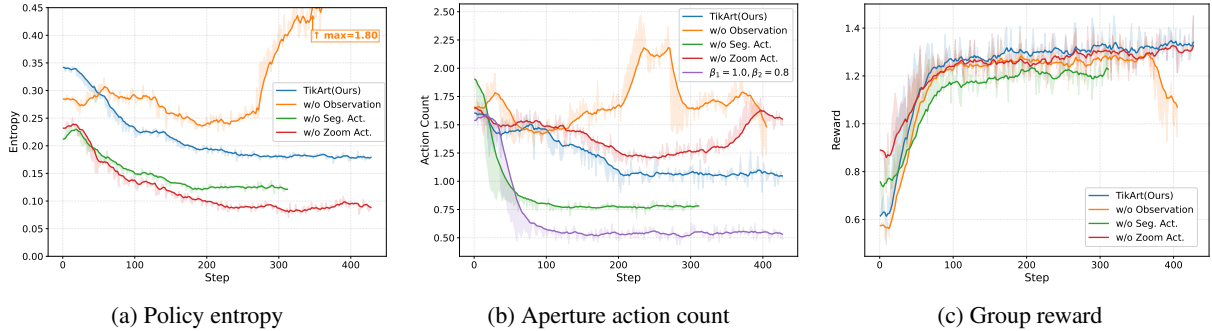


Figure 5: Training dynamics of TikArt and GRPO-based variants under AGRPO. We plot (a) policy entropy, (b) the average number of aperture actions per trajectory, and (c) group reward over training steps. TikArt converges to a stable policy with moderate entropy and a reasonable aperture usage rate, while removing Observation leads to exploding entropy (above 2.0), uncontrolled aperture actions, and degraded reward. The *w/o Segment Action* variant tends to under-use apertures, whereas the *w/o Zoom Action* variant becomes more deterministic with lower entropy. The purple curve corresponds to a variant with different reward weights ($\beta_1 = 1.0, \beta_2 = 0.8$), illustrating the impact of reward design. For other benchmarks, we evaluate the *w/o Observation* variant using its checkpoint at step 260, before the onset of training divergence.

els such as GPT-4o and Gemini-2.5 still hold a lead on some aggregate scores, TikArt substantially narrows the gap and, on multiple fine-grained categories involving local cues (e.g., object attributes, chart details), matches or exceeds their performance. These results suggest that aperture-guided observation benefits not only synthetic high-resolution benchmarks but also real-world high-resolution evaluation and broad multimodal understanding .

4.4 Segmentation

Table 3 reports segmentation performance of different vision–language models. TikArt-8B achieves the best ReasonSeg scores among all listed models while maintaining competitive RefCOCO performance. TikArt yields clear improvements over its backbone and other baselines, indicating that the learned region-of-interest policy naturally transfers from question answering to pixel-level grounding in complex scenes.

4.5 Ablation Studies

We conduct ablation studies to understand the contribution of aperture-guided observation. First, removing the **Observation** phase (i.e., the model still selects apertures but does not verbalize what it sees) leads to unstable training and a noticeable drop on V^* and HR-Bench, confirming that explicit observations are essential for both credit assignment and interpretability. Second, when we restrict the agent to a single aperture primitive, performance degrades on complementary cases. In

the *w/o Segment Action* variant, the model struggles with thin or irregular objects, while the *w/o Zoom Action* variant underperforms on structured layouts such as panels and tables. We also report a training-free baseline (*w/o GRPO*) that applies the TikArt prompts to Qwen3-VL-8B-Instruct at inference time. This prompt-only variant already brings non-trivial gains over the backbone, while full AGRPO training remains crucial for learning when and where to act. While iterative reasoning incurs overhead, our RL policy converges to a highly efficient strategy, averaging only 1.36 actions per trajectory on MME-RealWorld-Lite (Appendix A). Notably, ablating *Observation* increases latency, as the ungrounded agent fails to learn concise exploration.

5 Conclusion

In this paper, we introduce **TikArt**, a novel framework that enhances fine-grained visual reasoning in MLLMs through *aperture-guided observation*. By formalizing multimodal reasoning as a Markov Decision Process within a **Think–Aperture–Observe** loop, TikArt enables models to actively seek, isolate, and interpret critical visual details via unified Zoom and Segmentation actions. Optimized via AGRPO—a multi-stage reinforcement learning strategy that obviates the need for explicit chain-of-thought supervision—TikArt significantly outperforms its backbone and bridges the gap with much larger proprietary models on challenging high-resolution benchmarks like V^* and HR-Bench. Our results demonstrate that empowering MLLMs

with the agency to control their visual focus not only improves accuracy on intricate tasks but also yields interpretable reasoning trajectories, paving the way for more autonomous and precise multimodal agents.

Limitations

Note on fairness. Because TikArt performs iterative perception and may invoke an external segmenter, it can incur additional inference cost compared to single-pass MLLMs. We therefore report aperture usage statistics and latency, and we encourage evaluation under matched compute budgets when comparing tool-augmented and non-tool baselines.

Reliance on external segmentation backbones. Although our aperture policy is learned via RL, while calling a frozen SAM2, the segmentation action relies on an off-the-shelf SAM2 backbone to produce mask-based apertures, which makes TikArt’s performance partially dependent on SAM2’s accuracy, inductive biases, and prompt sensitivity. Since SAM2 is not jointly optimized with the language policy, systematic segmentation errors (e.g., fragmented masks, missed thin structures, or failures under severe occlusion and domain shift) can corrupt the returned RoI view and propagate to downstream reasoning, while being difficult to correct purely in the text domain. Moreover, invoking SAM2 introduces additional deployment complexity and inference-time overhead, and the need to predict box/point/label prompts adds an extra failure channel when spatial grounding is uncertain. Finally, our mask-based cropping (foreground highlighting with background suppression) may remove contextual cues that are useful for relational reasoning, suggesting a trade-off between object isolation and global context that future work could mitigate with more integrated or hierarchical visual front-ends.

Reinforcement learning cost and stability. Training TikArt with GRPO-style reinforcement learning over long multimodal trajectories is substantially more expensive than supervised fine-tuning. It requires sampling multiple trajectories per input, computing task and aperture-related rewards, and backpropagating through multiple aperture and observation steps. The learned policy can be sensitive to reward shaping, task mixture, and curriculum choices. While our two-stage training

procedure stabilizes learning for Qwen3-VL-8B, scaling TikArt to larger backbones, broader data, or richer action spaces may amplify these challenges.

Inference-time overhead. Aperture-guided reasoning incurs additional computational cost at inference time. Each aperture action requires processing an RoI, and segmentation actions invoke a heavyweight segmentation backbone. Although the learned policy tends to use a small number of apertures per trajectory, TikArt remains slower and more resource-intensive than single-pass MLLMs that operate on a fixed global encoding. This overhead may be problematic in latency-sensitive or resource-constrained settings. *We provide quantitative latency and aperture-usage statistics on MME-RealWorld-Lite in Appendix A (Fig. 6, Fig. 7, and Fig. 8).*

Limited action space and global context. TikArt currently uses a small set of cropping-like aperture actions (zoom and segmentation). This design is effective for fine-grained perception and reasoning segmentation, but it does not fully capture the richness of potential visual decisions (e.g., grouping multiple objects, simulating alternative viewpoints, or performing geometry-aware transformations). Moreover, repeated focusing on local apertures may bias the policy toward details at the expense of global context. Although the backbone retains the original image, there is no explicit mechanism to reason hierarchically across multiple spatial scales.

Backbone and benchmark coverage. Our experiments instantiate TikArt on a single 8B-scale backbone (Qwen3-VL-8B) and evaluate on a selected set of high-resolution, multimodal, and segmentation benchmarks. While the gains are consistent and substantial within this setup, it remains unclear how well aperture-guided observation transfers to other backbone families, parameter scales, or domains such as video and 3D perception. Additional evaluation is needed to assess robustness under stronger distribution shifts and long-horizon tasks.

References

Xiang An, Yin Xie, Kaicheng Yang, Wenkang Zhang, Xiuwei Zhao, Zheng Cheng, Yirui Wang, Songcen Xu, Changrui Chen, Chunsheng Wu, and 1 others. 2025. Llava-onevision-1.5: Fully open framework

for democratized multimodal training. *arXiv preprint arXiv:2509.23661*.

Jinze Bai, Shuai Bai, Yunfei Chu, Zeyu Cui, Kai Dang, Xiaodong Deng, Yang Fan, Wenbin Ge, Yu Han, Fei Huang, and 1 others. 2023. Qwen technical report. *arXiv preprint arXiv:2309.16609*.

Shuai Bai, Yuxuan Cai, Ruizhe Chen, Keqin Chen, Xionghui Chen, Zesen Cheng, Lianghao Deng, Wei Ding, Chang Gao, Chunjiang Ge, Wenbin Ge, Zhi-fang Guo, Qidong Huang, Jie Huang, Fei Huang, Binyuan Hui, Shutong Jiang, Zhaohai Li, Mingsheng Li, and 45 others. 2025. *Qwen3-vl technical report. Preprint*, arXiv:2511.21631.

Chao Chen, Zhixin Ma, Yongqi Li, Yupeng Hu, Yinwei Wei, Wenjie Li, and Liqiang Nie. 2025. *Reasoning in the dark: Interleaved vision-text reasoning in latent space. Preprint*, arXiv:2510.12603.

Lin Chen, Jinsong Li, Xiaoyi Dong, Pan Zhang, Yuhang Zang, Zehui Chen, Haodong Duan, Jiaqi Wang, Yu Qiao, Dahua Lin, and 1 others. 2024. Are we on the right way for evaluating large vision-language models? *Advances in Neural Information Processing Systems*, 37:27056–27087.

Gheorghe Comanici, Eric Bieber, Mike Schaeckermann, Ice Pasupat, Noveen Sachdeva, Inderjit Dhillon, Marcel Blistein, Ori Ram, Dan Zhang, Evan Rosen, and 1 others. 2025. Gemini 2.5: Pushing the frontier with advanced reasoning, multimodality, long context, and next generation agentic capabilities. *arXiv preprint arXiv:2507.06261*.

Deng-Ping Fan, Ming-Ming Cheng, Yun Liu, Tao Li, and Ali Borji. 2017. Structure-measure: A new way to evaluate foreground maps. In *Proceedings of the IEEE international conference on computer vision*, pages 4548–4557.

Jun Gao, Yongqi Li, Ziqiang Cao, and Wenjie Li. 2025. *Interleaved-modal chain-of-thought. Preprint*, arXiv:2411.19488.

Jack Hong, Chenxiao Zhao, ChengLin Zhu, Weiheng Lu, Guohai Xu, and Xing Yu. 2025. *Deep-EyesV2: Toward Agentic Multimodal Model. ArXiv:2511.05271 [cs]*.

Yushi Hu, Weijia Shi, Xingyu Fu, Dan Roth, Mari Os-tendorf, Luke Zettlemoyer, Noah A Smith, and Ranjay Krishna. 2024. *Visual sketchpad: Sketching as a visual chain of thought for multimodal language models. Preprint*, arXiv:2406.09403.

Jiaqi Huang, Zunnan Xu, Jun Zhou, Ting Liu, Yicheng Xiao, Mingwen Ou, Bowen Ji, Xiu Li, and Kehong Yuan. 2025. *Sam-r1: Leveraging sam for reward feedback in multimodal segmentation via reinforcement learning. Preprint*, arXiv:2505.22596.

Alexander Kirillov, Eric Mintun, Nikhila Ravi, Hanzi Mao, Chloe Rolland, Laura Gustafson, Tete Xiao, Spencer Whitehead, Alexander C. Berg, Wan-Yen Lo, Piotr Dollár, and Ross Girshick. 2023. *Segment anything. Preprint*, arXiv:2304.02643.

Xin Lai, Zhuotao Tian, Yukang Chen, Yanwei Li, Yuhui Yuan, Shu Liu, and Jiaya Jia. 2024. Lisa: Reasoning segmentation via large language model. In *Proceedings of the IEEE/CVF Conference on Computer Vision and Pattern Recognition*, pages 9579–9589.

Bangzheng Li, Ximeng Sun, Jiang Liu, Ze Wang, Jialian Wu, Xiaodong Yu, Hao Chen, Emad Barsoum, Muham Chen, and Zicheng Liu. 2025. *Latent visual reasoning. Preprint*, arXiv:2509.24251.

OpenAI. 2024. *Gpt-4o system card. Preprint*, arXiv:2410.21276.

OpenAI. 2025. *GPT-5 System Card. System card*, OpenAI. Accessed: 2026-01-04.

Martin L Puterman. 1990. Markov decision processes. *Handbooks in operations research and management science*, 2:331–434.

Nikhila Ravi, Valentin Gabeur, Yuan-Ting Hu, Ronghang Hu, Chaitanya Ryali, Tengyu Ma, Haitham Khedr, Roman Rädle, Chloe Rolland, Laura Gustafson, Eric Mintun, Junting Pan, Kalyan Vasudev Alwala, Nicolas Carion, Chao-Yuan Wu, Ross Girshick, Piotr Dollár, and Christoph Feichtenhofer. 2024. *Sam 2: Segment anything in images and videos. Preprint*, arXiv:2408.00714.

Zhihong Shao, Peiyi Wang, Qihao Zhu, Runxin Xu, Junxiao Song, Xiao Bi, Haowei Zhang, Mingchuan Zhang, Y. K. Li, Y. Wu, and Daya Guo. 2024. *Deepseekmath: Pushing the limits of mathematical reasoning in open language models. Preprint*, arXiv:2402.03300.

Zhaochen Su, Peng Xia, Hangyu Guo, Zhenhua Liu, Yan Ma, Xiaoye Qu, Jiaqi Liu, Yanshu Li, Kaide Zeng, Zhengyuan Yang, Linjie Li, Yu Cheng, Heng Ji, Junxian He, and Yi R. Fung. 2025. *Thinking with images for multimodal reasoning: Foundations, methods, and future frontiers. Preprint*, arXiv:2506.23918.

Gemini Team, Petko Georgiev, Ving Ian Lei, Ryan Burnell, Libin Bai, Anmol Gulati, Garrett Tanzer, Damien Vincent, Zhufeng Pan, Shibo Wang, Soroosh Mariooryad, Yifan Ding, Xinyang Geng, Fred Alcober, Roy Frostig, Mark Omernick, Lexi Walker, Cosmin Paduraru, Christina Sorokin, and 1118 others. 2024. *Gemini 1.5: Unlocking multimodal understanding across millions of tokens of context. Preprint*, arXiv:2403.05530.

Harsh Trivedi, Niranjan Balasubramanian, Tushar Khot, and Ashish Sabharwal. 2023. *Interleaving retrieval with chain-of-thought reasoning for knowledge-intensive multi-step questions. Preprint*, arXiv:2212.10509.

Haozhe Wang, Alex Su, Weiming Ren, Fangzhen Lin, and Wenhui Chen. 2025a. **Pixel reasoner: Incentivizing pixel-space reasoning with curiosity-driven reinforcement learning.** *Preprint*, arXiv:2505.15966.

Qixun Wang, Yang Shi, Yifei Wang, Yuanxing Zhang, Pengfei Wan, Kun Gai, Xianghua Ying, and Yisen Wang. 2025b. **Monet: Reasoning in Latent Visual Space Beyond Images and Language.** ArXiv:2511.21395 [cs].

Weiyun Wang, Zhangwei Gao, Lixin Gu, Hengjun Pu, Long Cui, Xingguang Wei, Zhaoyang Liu, Linglin Jing, Shenglong Ye, Jie Shao, Zhaokai Wang, Zhe Chen, Hongjie Zhang, Ganlin Yang, Haomin Wang, Qi Wei, Jinhui Yin, Wenhao Li, Erfei Cui, and 56 others. 2025c. **Internvl3.5: Advancing open-source multimodal models in versatility, reasoning, and efficiency.** *Preprint*, arXiv:2508.18265.

Wenbin Wang, Liang Ding, Minyan Zeng, Xiabin Zhou, Li Shen, Yong Luo, Wei Yu, and Dacheng Tao. 2025d. Divide, conquer and combine: A training-free framework for high-resolution image perception in multimodal large language models. In *Proceedings of the AAAI Conference on Artificial Intelligence*, volume 39, pages 7907–7915.

Penghao Wu and Saining Xie. 2024. V?: Guided visual search as a core mechanism in multimodal llms. In *Proceedings of the IEEE/CVF Conference on Computer Vision and Pattern Recognition*, pages 13084–13094.

Zhengyuan Yang, Linjie Li, Jianfeng Wang, Kevin Lin, Ehsan Azarnasab, Faisal Ahmed, Zicheng Liu, Ce Liu, Michael Zeng, and Lijuan Wang. 2023. **Mm-react: Prompting chatgpt for multimodal reasoning and action.** *Preprint*, arXiv:2303.11381.

Shunyu Yao, Jeffrey Zhao, Dian Yu, Nan Du, Izhak Shafran, Karthik Narasimhan, and Yuan Cao. 2023. **React: Synergizing reasoning and acting in language models.** *Preprint*, arXiv:2210.03629.

Zuyao You and Zuxuan Wu. 2025. **Seg-r1: Segmentation can be surprisingly simple with reinforcement learning.** *Preprint*, arXiv:2506.22624.

Licheng Yu, Patrick Poirson, Shan Yang, Alexander C. Berg, and Tamara L. Berg. 2016. **Modeling context in referring expressions.** *Preprint*, arXiv:1608.00272.

Qiyi Yu, Zheng Zhang, Ruofei Zhu, Yufeng Yuan, Xiaochen Zuo, Yu Yue, Weinan Dai, Tiantian Fan, Gao-hong Liu, Lingjun Liu, and 1 others. 2025a. **Dapo: An open-source llm reinforcement learning system at scale.** *arXiv preprint arXiv:2503.14476*.

Xuan Yu, Dayan Guan, and Yanfeng Gu. 2025b. **Zoom-refine: Boosting high-resolution multimodal understanding via localized zoom and self-refinement.** *Preprint*, arXiv:2506.01663.

Yi-Fan Zhang, Xingyu Lu, Shukang Yin, Chaoyou Fu, Wei Chen, Xiao Hu, Bin Wen, Kaiyu Jiang, Changyi Liu, Tianke Zhang, Haonan Fan, Kaibing Chen, Jiankang Chen, Haojie Ding, Kaiyu Tang, Zhang Zhang, Liang Wang, Fan Yang, Tingting Gao, and Guorui Zhou. 2025. **Thyme: Think Beyond Images.** ArXiv:2508.11630 [cs].

Yi-Fan Zhang, Huanyu Zhang, Haochen Tian, Chaoyou Fu, Shuangqing Zhang, Junfei Wu, Feng Li, Kun Wang, Qingsong Wen, Zhang Zhang, and 1 others. 2024. **Mme-realworld: Could your multimodal llm challenge high-resolution real-world scenarios that are difficult for humans?** *arXiv preprint arXiv:2408.13257*.

Ziwei Zheng, Michael Yang, Jack Hong, Chenxiao Zhao, Guohai Xu, Le Yang, Chao Shen, and Xing Yu. 2025. **DeepEyes: Incentivizing "Thinking with Images" via Reinforcement Learning.** ArXiv:2505.14362 [cs].

A Efficiency and Aperture Usage Statistics

This appendix complements the qualitative discussion of inference-time overhead by reporting (i) the distribution of the number of aperture actions per trajectory, (ii) the average aperture count, and (iii) the average inference time. **All statistics in this section are measured on the MME-RealWorld-Lite evaluation set** under the same evaluation protocol described in Appendix E. We focus on these statistics because TikArt may invoke additional computation beyond single-pass MLLMs: each aperture action requires processing an ROI, and segmentation actions may call a heavyweight segmentation backbone.

What is measured. We count the number of *aperture actions* taken within one trajectory (episode) and report its empirical distribution (Fig. 6). We also report the mean aperture count (Fig. 7) and the average end-to-end inference time (Fig. 8) on MME-RealWorld-Lite. Finally, to isolate the effect of aperture usage on runtime, we report the average inference time *conditioned on the number of aperture actions* (Fig. 9).

Key observations. First, TikArt concentrates on a small number of apertures per trajectory on MME-RealWorld-Lite, suggesting that the learned policy typically uses a limited number of zoom-in steps to gather evidence (Fig. 6). Second, removing the mandatory Observation phase substantially increases the average aperture usage (Fig. 7) and introduces a heavier tail with more frequent high-count trajectories (Fig. 6), indicating less controlled exploration. Finally, the increased aperture usage correlates with significantly higher latency on MME-RealWorld-Lite (Fig. 8), consistent with the fact that each additional aperture/segmentation step adds compute. This trend is further confirmed when we stratify runtime by aperture count: latency increases monotonically as the number of apertures grows (Fig. 9).

B Datasets and Settings

This appendix summarizes the main hardware, training and dataset hyperparameters used for GRPO alignment of Qwen3-VL-8B-Instruct on the TikArt tasks.

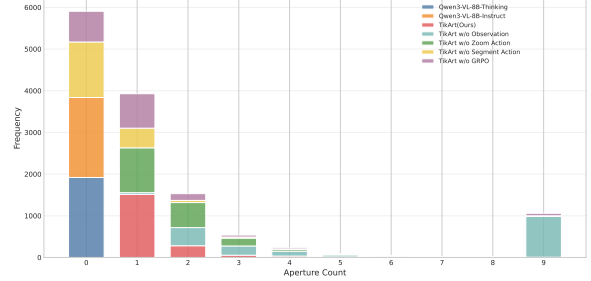


Figure 6: Distribution of the number of aperture actions per trajectory on MME-RealWorld-Lite (log-scale frequency). TikArt concentrates on a small number of apertures, while removing the mandatory Observation phase produces a heavier tail with more frequent high-count trajectories.

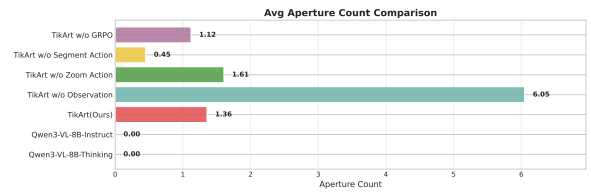


Figure 7: Average aperture count per trajectory on MME-RealWorld-Lite. TikArt uses 1.36 apertures on average, whereas the w/o Observation ablation increases this number to 6.05, suggesting that Observation helps regularize and stabilize purposeful aperture usage.

B.1 Training Configuration

Hardware and system. All GRPO experiments are conducted on a single node with 8 NVIDIA Tesla A100 GPUs. Distributed training uses DeepSpeed ZeRO Stage 3 with CPU offloading enabled for both model parameters and optimizer states. NCCL is used as the communication backend and the timeout is increased to 1,800 seconds (environment variable NCCL_TIMEOUT=1800000) to avoid failures during long GRPO iterations.

B.2 Training Datasets

Our full training pipeline follows a two-stage design, inspired by the data composition strategy described in DeepEyes and adapted to the needs of TikArt. In the first stage (Seg pre-training), we train the model exclusively on 2,000 segmentation-focused samples from COCO2017. This stage is designed to establish reliable competence in segmentation-oriented tool usage, including bounding box grounding, point-based prompting, and label recognition, mirroring the fine-grained perception emphasis observed in the Visual Search portion of the DeepEyes dataset. During this stage, the objective is not general vision-language rea-

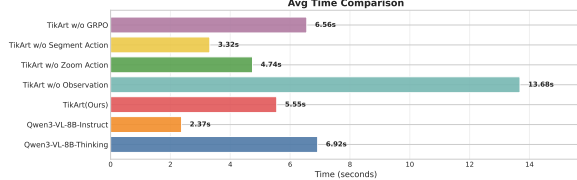


Figure 8: Average inference time (seconds) on MME-RealWorld-Lite. TikArt increases latency relative to the single-pass backbone (e.g., 5.55s vs. 2.37s for Qwen3-VL-8B-Instruct), and removing Observation further amplifies the cost (13.68s), consistent with increased aperture usage.

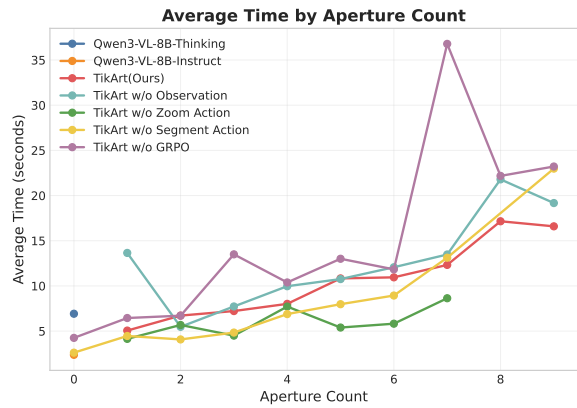


Figure 9: Average inference time (seconds) on MME-RealWorld-Lite conditioned on the number of aperture actions. Runtime increases monotonically with aperture count, reflecting the extra compute incurred by each additional ROI/segmentation step.

soning but rather ensuring that the model develops stable, consistent *w/o Zoom Action* variant invocation behavior.

In the second stage (multi-task training), we expand the data distribution to a mixture of perception, reasoning, and chart-style tasks. Following the structure of the DeepEyes corpus—where 47% of data targets fine-grained natural-image perception, 30% consists of chart understanding, and 23% focuses on multimodal reasoning—we construct a dataset comprising 40,000 randomly sampled instances from the DeepEyes-47K collection together with an additional 15,000 samples drawn from COCO2017, ReasonSeg(train split), and ADE20K. This multi-source mixture supports learning across three task families: visual mathematics, general visual question answering, and segmentation. The natural-image samples encourage precise visual grounding; the chart-like samples introduce abstract structured visual semantics; and the reasoning-oriented samples enhance robust-

ness across logical, numerical, and multi-step inference scenarios. This balanced composition follows the same design rationale as DeepEyes, where diverse visual distributions and reasoning styles help activate tool-aware multimodal reasoning capabilities. Our final mixed corpus thereby supports stable GRPO training while enabling the emergence of tool-integrated visual–linguistic reasoning.

C Discussion

C.1 Aperture-guided observation as a decision process

TikArt views multi-step visual reasoning as a Markov decision process over regions of interest (ROIs). Instead of relying on a single global encoding of the image, the agent repeatedly selects *apertures*—localized ROI crops that act as controllable windows of visual focus—and updates its internal state based on what is observed there. This formulation brings the model closer to human visual cognition, where reasoning proceeds through a sequence of fixations and saccades over informative parts of the scene rather than a single holistic glance.

In this MDP view, three components become explicit: (i) the state, which combines the original image, the textual query, the history of language tokens, and previously inspected apertures; (ii) the action, which decides where and how to place the next aperture; and (iii) the observation, a natural-language description of the selected region. The Think–Aperture–Observe loop we adopt makes all three observable, allowing us to inspect how the model trades off between exploring new ROIs and exploiting already collected evidence.

C.2 Zoom and segmentation as unified aperture actions

Although TikArt must operate across diverse visual regimes (icons and panels in high-resolution benchmarks, cluttered objects in natural images, and pixel-level masks in reasoning segmentation), it uses a compact set of *aperture actions*. The *zoom* action corresponds to directing foveal vision toward a bounded ROI, such as a diagram panel, a table cell, or a small object. The *segmentation* action corresponds to delineating irregular or overlapping foreground regions, akin to mentally tracing the outline of an object or a group of objects; in practice this is instantiated by a segmentation backbone (e.g., SAM2).

From the agent’s perspective, both actions are instances of the same underlying decision: *where to attend next and at what granularity*. This unification is important for training, as it allows a single policy to coordinate structured and free-form RoIs. Empirically, we find that zoom is often used to localize coarse spatial structure (e.g., selecting a relevant panel or region), while segmentation refines the focus around thin structures or small, densely packed objects that are difficult to isolate by rectangular crops alone. The learned policy typically uses only a few apertures per trajectory, suggesting that the agent discovers efficient strategies for combining these actions.

C.3 The role of explicit observation

A central design choice in TikArt is the mandatory Observation phase after every aperture action. Rather than treating visual operations as latent, the agent must explicitly verbalize what appears in the selected ROI before continuing to reason. This has two key effects.

First, observations act as persistent memory: once a local detail is described in language, it becomes available to all subsequent steps, even if the corresponding aperture is no longer active. This is particularly beneficial on benchmarks such as V* and HR-Bench, where the answer often depends on aggregating cues from multiple small regions. Second, the observation requirement regularizes the policy space. The agent cannot silently apply arbitrary visual transforms; each aperture must be justified by a linguistic description that is consistent with the question and previous context. Our ablations show that removing explicit observations leads to unstable reinforcement learning and notable drops in fine-grained perception, indicating that observation is not just an explanatory layer but an essential part of the decision-making loop.

C.4 Empirical behavior and interpretability

Across benchmarks, we observe qualitatively meaningful aperture trajectories. On high-resolution visual reasoning tasks, TikArt often first zooms into coarse structural regions (e.g., the relevant panel in a multi-panel figure), then iteratively refines its focus via smaller zooms or segmentation actions to isolate critical details. On reasoning segmentation tasks such as ReasonSeg, aperture decisions correlate with “stepwise grounding”: the agent first identifies the logical subscene referenced by the text, then segments the object or region that matches the

current reasoning hypothesis.

These trajectories are inherently interpretable: each action is anchored to a visible ROI, and each ROI is accompanied by an observation that explains what the model believes it sees. This stands in contrast to purely latent or text-only chains of thought, where intermediate visual decisions are inaccessible. The interpretability of aperture-guided observation is useful both for diagnosing model failures (e.g., mis-localization vs. mis-reasoning) and for understanding emergent behavior such as when and why the agent chooses not to use apertures at all.

C.5 Relation to concurrent paradigms

Recent work has explored interleaved multimodal chains-of-thought and latent visual reasoning. Some methods acquire auxiliary images or crops via coordinate prediction and external tools, while others reason directly in a latent visual space without explicit ROIs. TikArt lies between these extremes: it maintains a concrete, image-space notion of ROIs through apertures, but learns *when* and *how* to invoke them via reinforcement learning rather than hard-coded workflows. Compared to pipeline-style approaches, this yields more flexible and task-dependent aperture usage; compared to latent-only approaches, it offers stronger interpretability and a direct connection to pixel-level grounding (e.g., segmentation masks).

D Future Work

Toward more integrated visual front-ends. An important direction is to reduce the reliance on external segmentation modules by integrating more of the visual front-end into the MLLM itself. Possible approaches include distilling the segmentation backbone into the vision encoder, jointly training the aperture policy and segmentation layers, or moving toward latent segmentation where ROIs are represented implicitly in the model’s hidden space. Such integration could improve robustness, simplify deployment, and avoid discrepancies between open- and closed-source pipelines.

More expressive aperture actions. Extending the action space beyond simple crops is another promising direction. For example, future work could explore hierarchical apertures (coarse-to-fine ROIs), multi-object apertures, or actions that manipulate viewpoint and geometry. In video and 3D settings, temporal or volumetric apertures may allow the agent to decide not only where to look,

but *when* and *from which perspective*. Designing such actions while keeping reinforcement learning tractable is an open challenge.

Improved RL algorithms and credit assignment. TikArt currently relies on GRPO with relatively simple reward shaping. More advanced RL techniques tailored to multimodal reasoning—such as better credit assignment across aperture and language tokens, off-policy or offline RL with replay, or multi-objective optimization balancing accuracy and computation—could further improve sample efficiency and stability. Exploring the interaction between supervised pre-training, self-imitation, and RL for aperture policies is another promising avenue.

Adaptive computation and distillation. To mitigate inference-time overhead, future work could incorporate adaptive aperture budgets, early-exit criteria based on confidence, or dynamic policies that fall back to single-pass reasoning when apertures are unlikely to help. Another complementary direction is to distill TikArt’s aperture-guided behavior into a cheaper student model that imitates successful trajectories without executing all aperture actions at test time.

Bridging explicit apertures and latent visual reasoning. Finally, it would be interesting to connect explicit aperture-guided observation with latent visual reasoning paradigms that operate directly in embedding space. One possibility is to let the agent choose between concrete image-space apertures and latent “visual thoughts” depending on the task, treating both as actions in a unified policy. Such a hybrid design could combine the interpretability and grounding benefits of explicit RoIs with the flexibility of latent visual computation, potentially leading to even stronger fine-grained and abstract visual reasoning.

E Prompts

E.1 TikArt

TikArt – System Prompt

```
You are a helpful assistant
# Tools
You may call the segmentation or zoom
function to extract specific
regions from images.
Function signature provided within <
tools></tools> XML tags:
<tools>
```

```
{"type": "function", "function": {
  "name": "image_segment_tool",
  "description": "Generate a
    segmentation mask for specified
    region, mask non-target areas as
    Gaussian noise, and crop using
    bounding box",
  "parameters": {"type": "object", "properties": {
    "bbox": {"type": "array", "items": {"type": "number"}, "minItems": 4, "maxItems": 4,
    "description": "Bounding box as [x1,
      y1, x2, y2]"},
    "points": {"type": "array", "items": {"type": "array", "items": {"type": "number"}, "minItems": 2, "maxItems": 2,
    "description": "List of point
      coordinates"},
    "labels": {"type": "array", "items": {"type": "integer"},
    "description": "Labels for each point
      (1=foreground, 0=background)"}
  },
  "obj_label": {"type": "string",
    "description": "Optional object
      name"}},
  "required": ["bbox", "points", "labels"]
}}
</tools>

<tools>
{"type": "function", "function": {"name": "image_zoom_in_tool", "description": "Zoom in on a specific
  region of an image by cropping it
  based on a bounding box", "parameters": {"type": "object", "properties": {
    "bbox": {"type": "array", "items": {"type": "number"}, "minItems": 4, "maxItems": 4,
    "description": "Bounding box [x1, y1,
      x2, y2]"},
    "obj_label": {"type": "string",
      "description": "Optional object name
      "}},
    "required": ["bbox"]}}
</tools>

# How to call a tool
Return a json object with function
name and arguments inside <
tool_call></tool_call>:

<tool_call>
{"name": <function-name>, "arguments": <args-json-object>}
</tool_call>

Examples:
<tool_call>
{"name": "image_segment_tool",
  "arguments": {"bbox": [100, 80, 450,
    400],
    "points": [[300, 180], [280, 200]], "labels": [1, 0], "obj_label": "Cat
    "}},
  </tool_call>
```

```

<tool_call>
{"name": "image_zoom_in_tool",
"arguments": {"bbox": [10, 20, 100, 200], "obj_label": "the apple on
the desk"}}
</tool_call>

# Tool Rules
- Only one tool can be called per turn
.
- You must print your thinking process
step by step before calling a
tool.

Think first, call **image_segment_tool**
** or **image_zoom_in_tool** if
needed, then answer.

```

TikArt – User Prompt

Describe what you observe in this response first, then think step by step.
Call **image_segment_tool** or **image_zoom_in_tool** if needed, then answer.

Format as:
Image Description here...
Thinking Process here...
<tool_call>...</tool_call> (if tools needed)
<answer>(If no tools needed, Answer here...) </answer>

E.2 w/o observation

w/o observation – User Prompt

Think step by step first, call **image_segment_tool** or **image_zoom_in_tool** if needed, then answer.

Format as:
(Thinking Process)
<tool_call>...</tool_call> (if tools needed)
<answer>(If no tools needed, Answer here...) </answer>

TikArt w/o Segment Action

Zoom – System Prompt

You are a helpful assistant
Tools
You may call the zoom function to
extract specific regions from
images.
Function signature provided within <
tools></tools>:

<tools>

```

{"type": "function", "function": {"name": "image_zoom_in_tool",
"description": "Zoom in on a region by
cropping with a bounding box",
"parameters": {"type": "object", "properties": {}},
"bbox": {"type": "array", "items": {"type": "number"}, "minItems": 4, "maxItems": 4,
"description": "Bounding box [x1, y1, x2, y2]"},
"obj_label": {"type": "string", "description": "Optional object name
"}},
"required": ["bbox"]}}
</tools>

```

Tool Rules
- Only one tool can be called per turn
.
- You must print your thinking process
step by step before calling a
tool.

Think first, call **image_zoom_in_tool**
** if needed, then answer.

Zoom – User Prompt

Think step by step first, call **image_zoom_in_tool** if needed, then answer.

Format as:
(Thinking Process)
<tool_call>...</tool_call>
<answer>(If no tools needed, Answer here...) </answer>

E.3 TikArt w/o Zoom Action

Segment – System Prompt

You are a helpful assistant
Tools
You may call the segmentation function
to extract specific regions from
images.
Function signature provided within <
tools></tools>:

```

<tools>
{"type": "function", "function": {"name": "image_segment_tool",
"description": "Generate a
segmentation mask for specified
region",
"parameters": {"type": "object", "properties": {}},
"bbox": {"type": "array", "items": {"type": "number"}, "minItems": 4, "maxItems": 4,
"points": {"type": "array"}, "labels": {"type": "array"}, "obj_label": {"type": "string"}},
"required": ["bbox"]}}
</tools>

```

```

"required":["bbox","points","labels
"]}}}
</tools>

# Tool Rules
- Only one tool can be called per turn
.
- You must print your thinking process
  step by step before calling a
  tool.

Think first, call **image_segment_tool
** if needed, then answer.

```

Segment – User Prompt

Think step by step first, call **
 image_segment_tool** if needed,
 then answer.

Format as:
 (Thinking Process)
 <tool_call>...</tool_call>
 <answer>(If no tools needed, Answer
 here...) </answer>

E.4 TikArt w/o GRPO

This is a training-free (prompt-only) variant: we directly run Qwen3-VL-8B-Instruct with the same TikArt prompts as in Appendix E.1, without any AGRPO fine-tuning.